LUMEN Thrust Chamber - Injector Design and Stability Analysis

By Justin HARDI,[1)] Jan DEEKEN,[1))] Wolfgang ARMBRUSTER,[1))] Yannik MIENE,[1))] Jan HAEMISCH,[1))] Jan MARTIN,[1))] Dmitry SUSLOV,[1)] and Michael OSCHWALD[1),2)]

[1)]*Institute of Space Propulsion, DLR, Hardthausen, Germany*

[2)]*Institute of Jet Propulsion and Turbomachinery, RWTH Aachen University, Aachen, Germany*

(Received June 21st, 2019)

The LUMEN project at the DLR Institute of Space Propulsion has the goal of producing a bread-board demonstrator engine powered by LOX/LNG. This paper describes the design of the baseline injection system for the LUMEN thrust chamber which uses the advance porous injector (API) concept. Numerical analysis of internal flow characteristics and acoustics of the injector used in the design phase are presented. The injection system was designed to avoid injection-coupled combustion instabilities. A prediction of the low-frequency stability characteristics is also presented.

Key Words: LUMEN demonstrator, injector design, stability analysis

1. Introduction

The LUMEN project at the German Aerospace Center (DLR), Institute of Space Propulsion has the goal of producing a bread-board demonstrator engine powered by LOX/LNG.[8)] The engine features an expander bleed cycle, an advance porous injector (API),[2,10,24,30)] and a laser ignition system.[3)] Initial testing of the new injector design is currently underway at the European Research and Technology Test Facility P8 for cryogenic rocket engines at the DLR Lampoldshausen site. This article provides an overview of the design of the LUMEN injection system and its predicted performance.

The LUMEN breadboard engine is designed to operate over a wide range of operating conditions. The operational envelope is defined by a pressure range of 35 to 80 bar and a propellant mixture ratio range of 3.0 to 3.8. The nominal point is defined as a mean combustion chamber pressure (p_{CC}) of 60 bar and ratio of oxidiser to fuel mass flow rate (ROF) of 3.4. The LUMEN requirements call for an injection system which

- provides stable combustion of LOX/LNG over the whole operational domain with a maximum allowable combustion roughness (RMS) of 2.5% of p_{CC},
- provides stable combustion with a maximum pressure drop of $\Delta p_{LOX} = 15\% p_{CC}$ and $\Delta p_{LNG} = 10\% p_{CC}$,
- provides combustion efficiency in excess of 95% at nominal conditions with the shortest possible combustion chamber length,
- provides the necessary heat flux to the chamber walls to cover the power requirements of the two LUMEN turbines with the shortest possible combustion chamber length, and
- is compatible with a cylindrical chamber diameter of 80 mm.

Due to the existing heritage in injector technology at DLR, two concepts were considered for the LUMEN injector: classical shear-coaxial injectors and the advanced porous injector (API). The favorable characteristics of API with respect to combustion efficiency, operation at low injection pressure drop, and its distinct wall heat flux distribution[10)] made this concept the preferred choice for the LUMEN system. Nevertheless, a shear-coaxial injector design will serve as a back-up solution for the project.

The occurrence of injection coupled combustion instabilities during transient and/or steady-state operation is considering the largest technological risk for the development of the LUMEN injection system. Therefore, the injector design process focused largely on measures to avoid injection-coupled combustion instabilities.

The problem of combustion instabilities has troubled many engine development programmes throughout the history of liquid rocket engines (LREs).[17,33)] Predicting and preventing high-frequency combustion instability is a difficult task, because the detailed coupling mechanisms leading to the dangerous pressure oscillations are usually not fully understood and in most cases are hard to identify. In the 1960s the investigation of combustion instabilities in the US J2-S engine was one of the first cases in which coupling of chamber modes with LOX-post acoustics was identified as the driving mechanism.[20)] Since then, LOX-post coupling has been identified in more and more cases from single-element experiments using LOX/H_2[26,27)] and LOX/CH4,[22)] as well as multi-element sub-scale chambers,[13,19,21,22,25)] through to the recent Japanese main stage demonstrator engine LE-X.[32)] From the scope of published examples it can be seen that LOX-post coupling is a prevalent potential source of high-frequency combustion instabilities in cryogenic rocket engines. Recent work as DLR has focussed on the measurement and prediction of injection coupled instabilities, and so the developed methodology was applied in the design phase of the LUMEN injector.

This article presents the injection system for LUMEN. First, the selected design of the injector is described, and the distribution of LOX among the injection posts is analysed with CFD. Then, the acoustic modes of the injector and combustion chamber are estimated and the potential for coupling of the resonance systems is assessed. This is supplemented with an acoustic modal analysis of the injector head to check if distribution volumes could be a source of resonant coupling. Finally, low frequency stability characteristics are estimated with the well-

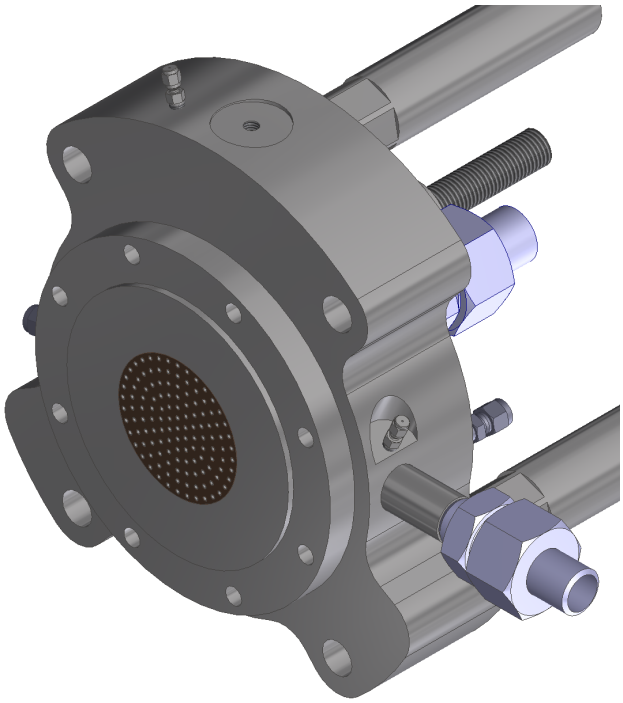

Fig. 1. CAD model of the LUMEN porous injector head.

known modelling approach from Crocco.

2. Injector head design

2.1. Porous injector

The design of the LUMEN injection system is driven by the propellant inlet conditions defined by the engine cycle. The LUMEN breadboard demonstrator is an expander bleed cycle with partial fuel remixing, similar to the LE-5B LOX/LH_2 engine. Part of the heated coolant flow is remixed into the main fuel mass flow to the injector, thus raising the injection temperature above the pump outlet temperature. The target injection conditions for the nominal load point are given in Table 1.

Table 1. Injection conditions for the LUMEN injector at nominal conditions.

	Unit	Value
Chamber pressure	bar	60
Chamber fuel mixture ratio	-	3.4
LOX mass flow rate	kg/s	5.95
LNG mass flow rate	kg/s	1.75
LOX injection temperature	K	98
LNG injection temperature	K	215

The porous injector arrangement designed for the LUMEN demonstrator consists of 127 LOX injectors and a porous face plate for LNG injection covering the entire chamber cross section of 80-mm diameter. The porous face plate itself is divided into three plates of 12-mm thickness which are made of a sintered steel mesh.

The inner injector cartridge is located in a massive main body of the injector head which also provides the mechanical interfaces to the P8 test facility and the downstream thrust chamber components. The LUMEN injector design is depicted in Fig. 1.

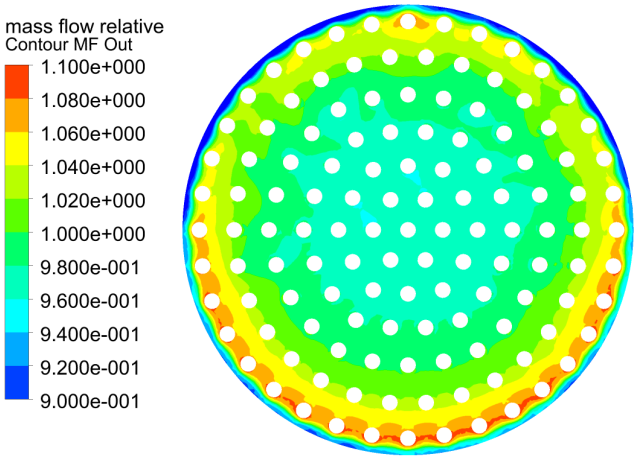

Fig. 2. Relative LNG mass flow rate at the outlet of the porous face plate (injection plane).

2.2. CFD analysis

For a homogeneous distribution of injected ROF, an even mass flow distribution of propellant to each injector element is crucial. Moreover, a non-uniform distribution can lead to combustion instabilities.[6] The uniformity of injector mass flow was evaluated numerically using the commercial software ANSYS CFX 18.0 for LOX and LNG side, respectively.

While the LOX injector pattern exhibits a 60 degree symmetry, the LOX side had to be modelled as a 180-degree section to capture the influence of internal elements with a different symmetry. For the nominal operating condition the numerical results indicate a maximum mass flow deviation of 5.58% for the LOX side. The median value for the deviations is about 1.77%. These deviations are considered to be acceptable.

The fuel side was modelled in full 360 degrees and used a fluid as well as a porous domain to simulate the correct crosswise mass flow inside the porous media. The necessary permeability parameters were calculated from earlier tests with the same face plate material. The resulting mass flow deviation are shown for the nominal condition in Fig. 2. For the largest part of the face plate area, the absolute mass flow deviation is well below 5%. Only the outer row of LOX injectors is located in a face plate area where higher LNG mass flow rates can be expected. In this region, the calculated relative mass flow ranges from 94% at the chamber wall to about 108% of the mean mass flow rate in the vicinity of the outer row of LOX injectors. The outer row of LOX injectors can therefore be expected to operate at a slightly lower mixture ratio.

A similar analysis has previously been performed for the 'L42' injector head at DLR. L42 has 42 shear coaxial injector elements. The LOX manifold is designed to achieve a uniform mass flow distribution. The design process was mainly guided by CFD simulations performed with the commercial software ANSYS CFX 18.0.

Figure 3 shows the pressure distribution inside the LOX manifold from such a simulation. The flow enters from the left side and spreads around the circumference of an outer distribution ring. The fluid then enters the main manifold that narrows to the centre. One can see that the pressure distribution is already very even. The LOX then passes through a distribution plate and comes into another manifold where it finally enters the in-

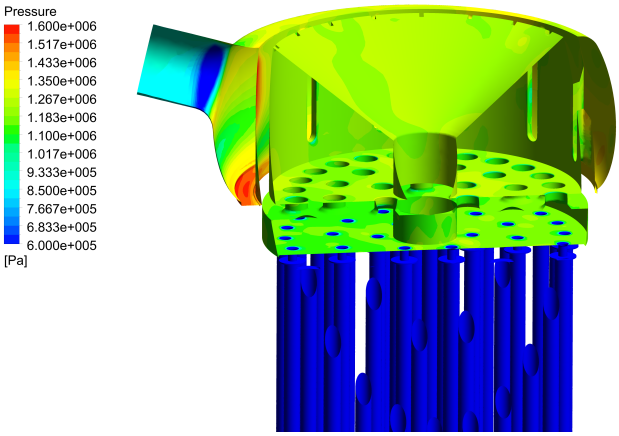

Fig. 3. Pressure distribution in the LOX manifold.

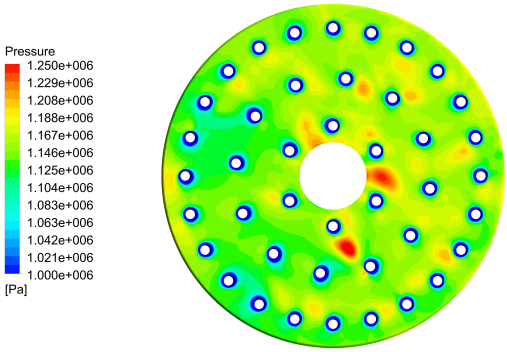

Fig. 4. Pressure distribution onto the final throttling plate.

jection elements.

Figure 4 shows the pressure distribution on this plate. The small pressure peaks between some of the injection elements are due to jets that are formed by the holes of the upstream distribution plate. The pressure distribution at the elements themselves on this plane is very even and therefore also the mass flow distribution. The deviation between elements is less then 2% of the average mass flow.

This result has been validated by tests with water as a substitute for LOX that were performed after manufacture and prior to combustion tests. Figure 5 shows the experimental setup. The flow of water through each injection element is collected in a separate canister. These canisters are weighed to calculate the average mass flow for each injector. The total volume flow is measured with a turbine flow meter and a pressure sensor displays the pressure loss.

The CFD approach is considered to be well validated by such tests. This provides confidence in the calculation of the LUMEN injector head, although a similar experimental measurement has not yet been performed.

3. Injector head acoustic analysis

Past experience at DLR has demonstrated how the acoustic resonance modes of injection manifolds can be unexpectedly excited and cause unwanted injection oscillations.[16] It was also shown how a fully detailed acoustic model of the injectors and coupled volumes can be used to predict and design remedies for such effects. To assess the potential for resonance in the LUMEN injector head, a modal analysis of the LOX injection

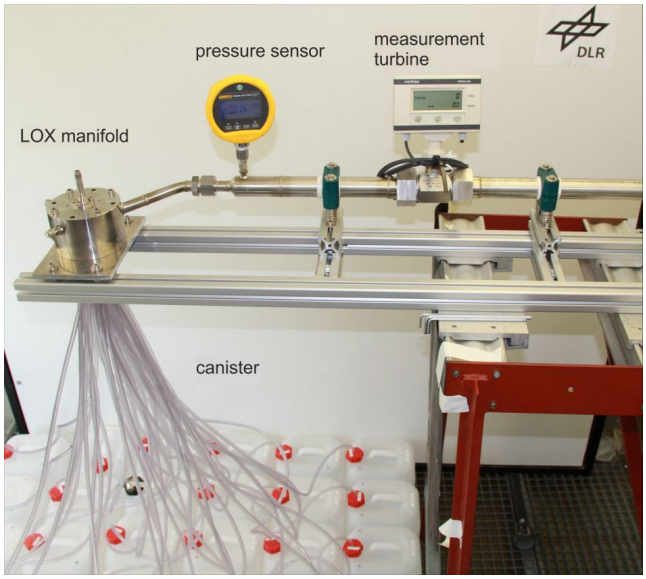

Fig. 5. Experimental setup to measure the mass flow distribution of the injection elements with water.

system was performed in COMSOL Multiphysics.

Using the pressure acoustics interface in the frequency domain, a full 3D model was created for the LOX injection volumes and posts with a tetrahedral mesh consisting of 2.5 million elements. Material properties for the linear-elastic fluid model were taken from REFPROP[23] for the nominal load point at 60 bar chamber pressure. The exits of the injectors into the chamber volume were considered sound soft, while all other boundaries were treated as a hard wall. With only low Mach numbers in the LOX system, background flow was considered negligible. The Helmholtz Eigenfrequency solver was used to find the resonance modes of the system.

Several coupled modes in the manifolds and injectors could be identified. Some could be considered dangerous because the amplitude in the manifold and injectors were close, for example for the manifold first tangential (1T), post first longitudinal (1L) coupled mode shown in Fig. 6. With the estimated 1T mode of the chamber in the same frequency range as this and other transverse modes of the LOX manifold, they were considered to present a risk to combustion stability.

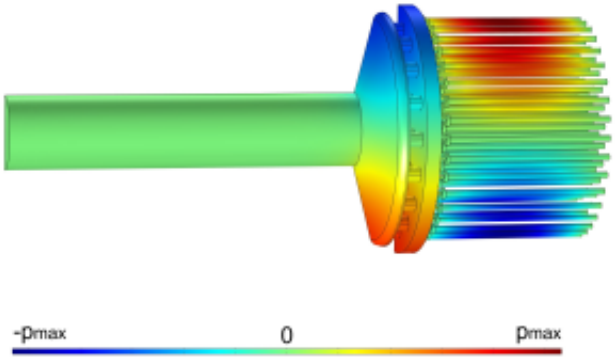

Fig. 6. Coupled longitudinal tangential mode of the initial LUMEN LOX injection system with the FEA acoustic model.

It was therefore considered prudent to implement a countermeasure. A baffle design was implemented into the LOX pre-

injection volume. The model geometry was updated and the analysis repeated. The damping effect of the baffles cannot be estimated due to the inviscid fluid model. However, the impact of the baffle on the pressure distribution and frequency resulted in a reduction in the amplitude in the manifold volume by about 25% relative to the LOX posts. Past experience at DLR with similar measures in another experimental combustor[16] provide confidence that it will be effective.

In order to investigate LOX-injection coupling, the longitudinal LOX post mode frequencies were obtained from the COMSOL results for the full LOX system model. The 1L of the LOX posts has a frequency of 6.6 kHz with the pressure distribution shown in Fig. 7. The post mode frequencies will be compared to combustion chamber mode frequencies in the next section.

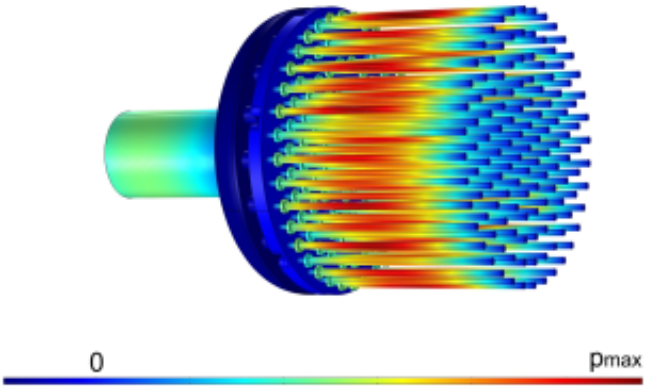

Fig. 7. LOX post 1L mode of the updated LUMEN injection system with the FEA acoustic model.

4. Thrust chamber coupled acoustics

The potential for acoustic coupling between the chamber and LOX posts was addressed early in the design phase of the LUMEN injector head. Whereas identifying LOX-post coupling in experimental data has already been realised by several research groups, it is a difficult task to accurately predict chamber and injector frequencies in order to assess the potential for injection-coupling in a new thrust chamber. The approach taken for LUMEN is explained in this section.

4.1. Combustion chamber acoustic model

A common method to predict the frequencies of the chamber acoustics is to simplify the combustion chamber as a closed cylinder and use the analyitcal equation for cylinder aocustics, as given in Eq. 1, where R is the radius and L the length of the chamber. Here, m, n, and q are integer variables for radial, tranverse and longitudnal modes. Combination modes are also possible. The values for α_{mn} are given in Table 2.[12]

$$f = \frac{c_{CC}}{2}\sqrt{\left(\frac{\alpha_{mn}}{R}\right)^2 + \left(\frac{q}{L}\right)^2}. \quad (1)$$

The speed of sound of the combustion products in the combustion chamber (c_{CC}) can be estimated with NASA CEA ($c_{CC,CEA}$). However, using this value in Eq. 1 assumes uniform

Table 2. Values for α_{mn}

α_{mn} n/m	0	1	2	3
0	0	1.220	2.333	3.238
1	0.586	1.697	2.717	3.726
2	0.972	2.135	3.173	4.192
3	1.337	2.551	3.612	4.643
4	1.693	2.995	4.037	5.082

c_{CC} in products at chemical equilibrium. Furthermore, Eq. 1 neglects the influence of flow through the chamber, both assumptions leading to inaccuracy in the calculated mode frequencies. In various experiments it was observed that the measured frequencies vary from those predicted by Eq.1. In Russia this discrepancy was attributed to a "cold zone" close to the injector faceplate where the relatively cold propellants are injected and have to be atomised, mixed and combusted until chemical equilibrium is achieved.[11]

Due to the length of the combustion zone the effective c close to the injector face plate is lower than at the end of the combustion zone. Reductions of 15% to 30% have been published.[11,14,19,21] Nevertheless, this reduction depends on multiple parameters such as the length of the combustion zone, the combustion efficiency, the temperature of the injected propellants and the geometry of the combustion chamber.

Greatly improved accuracy of the chamber frequencies can be realised with fully 3D numerical simulations. This has already been shown for a multi-element DLR combustion chamber.[31] Nevertheless, this approach requires an extreme amount of computational resources and is therefore currently regarded as infeasible for the stability analysis of a LRE during its development phase in which changes in the geometry and the operating conditions are likely to occur. At TU Munich, a hybrid CFD/CAA approach is used, where a single flame is modelled with CFD and the radially averaged sound speed profile is then applied to a 3D linearised Euler equation (LEE) solver.[29] A similar methodology has also successfully been used by DLR and ArianeGroup.[15]

A typical radially averaged axial c_{CC} profile for LOX/H_2 combustion is shown in Fig. 8. As can be observed, the c_{CC} distribution leads to a reduced effective c_{CC} in the range of the combustion zone $\bar{c}_{cz}$ and also over the full length of the chamber $\bar{c}$. Here, the length of the combustion zone can be defined as the length before the final plateau of c_{CC} where chemical equilibrium is reached. Usually the transverse modes inhabit the region close to the injector and are therefore mainly influenced by $\bar{c}_{cz}$, whereas longitudinal modes are influenced by $\bar{c}$. For LOX/H_2, the ratio $k_l = \bar{c}/c_{max}$ was typically in the range of about 0.9-0.95 and $k_t = \bar{c}_{cz}/c_{max}$ around 0.8-0.88. However, these values depend on many parameters including the injection conditions and the length of the chamber.

For the development of the LUMEN injector head, there was no CFD solution of the flame available at the time this acoustic analysis was required. Therefore, the approach was simplified to approximate the influence of the c_{CC} distribution in the chamber using a choice of appropriate k_l and and k_t factors. The influence of flow in the chamber was simplified to a uniform, mean axial flow, and both adjustments were implemented in the

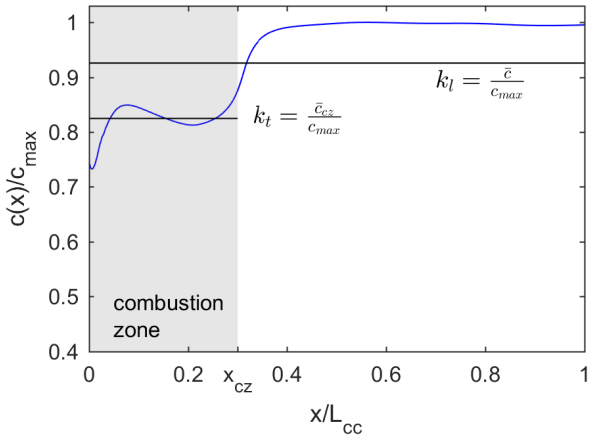

Fig. 8. Typical radially averaged speed-of-sound profile of a DLR LOX/H_2 combustion chamber calculated with the DLR flow solver TAU, adapted from.[15)]

analytic equation for mode frequencies in a cylindrical volume:

$$f = \frac{c(\eta_{c*})}{2}\sqrt{\left(\frac{\alpha_{mn}}{R}\right)^2(1-\bar{M}a^2)k_t^2 + \left(\frac{q}{L}\right)^2(1-\bar{M}a^2)^2k_l^2}. \tag{2}$$

4.2. Injector acoustic model

Compared to the combustion chamber acoustics, the estimation of LOX-post mode frequencies is simpler because the fluid properties inside the injector are well defined. The expected LOX temperature for the LUMEN nominal load point at 60 bar is 97.9 K,[9)] with fluid properties from NIST REFPROP 9.1[23)] of c_{LOX} = 872.3 m/s and ρ_{LOX} = 1116.8 kg/m^3.

The simplest estimate of the longitudinal mode frequencies is obtained by approximating the LOX post as an open-open tube. Previous experimental measurements from a DLR LOX/H_2 research combustor showed that this assumption gives acceptable accuracy.[13)] Since the Mach number of the LOX flow in the post is less than 0.02, the assumption of a standing mode holds. Therefore, the mode frequencies can be calculated with

$$f_{nL} = \frac{nc_{LOX}}{2L}. \tag{3}$$

In literature an end correction of $\Delta L = 0.8d$ is added to the injector length,[11)] leading to

$$f_{nL} = \frac{nc_{LOX}}{2(L+\Delta L)}. \tag{4}$$

Another possibility would be to use published experimentally measured wave numbers of LOX posts of a DLR research combustor of similar scale[13)] and adjust them according to the LUMEN injector length. However, these simplified methods do not account for specific geometrical features of the LUMEN injectors. The previously described FEA acoustic modelling of the injector head captures the influence of such features. However, the influence of flow is neglected, which will have an impact especially at area changes in the injector.

In order to account for both geometrical and flow effects in the LOX posts, an acoustic network model was used. Acoustic network models are often used in the stability analysis of gas turbine combustors[18,28)] and LREs.[1,12,29)] The acoustic network model is based on linear acoustic theory and only plane waves in axial directions of the injectors are considered. Therefore the complex geometry of the injector head has to be decomposed into an arrangement of simple acoustic elements. Transfer matrices for different types of elements, such as a straight tube or a sudden area change, can be found in literature.[18,28)] Analytic solutions for the wave propagation in the elements exists in terms of the Riemann invariants with the f wave travelling in positive direction and g in negative direction. Finally a system matrix S including the individual transfer matrices of each element can be formed. The resonance modes of the system are calculated by finding the eigenvalues of

$$\det(S(\omega)) = 0. \tag{5}$$

with

$$S = \begin{bmatrix} T_{fg,1} & \dots & 0 \\ \vdots & \ddots & \vdots \\ 0 & \dots & T_{fg,n} \end{bmatrix}. \tag{6}$$

A network model of a single LUMEN LOX injector was constructed. A simplified one-dimensional flow solver assuming isentropic flow is used to estimate the axial distribution of Mach number and pressure, with rho_{LOX} and c_{LOX} from REFPROP. The exit of the post was set as acoustically open. Fig. 9 shows the resulting acoustic pressure distribution of the LOX post 2L mode calculated with the acoustic network model for different phases of the oscillation.

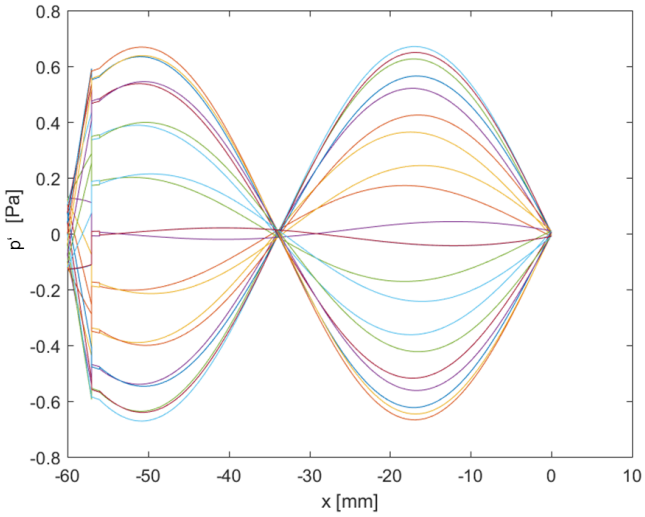

Fig. 9. Acoustic pressure distribution of the LOX post 2L mode calculated with the acoustic network model.

Table 3 summarises the calculated 1L and 2L LOX post frequencies for the different methods. Although the LOX post acoustics seem to be simpler than in the combustion chamber, there are discrepancies between the different methods up to ±6%. Only the network model and the FEA take into account the geometry of the LUMEN injectors, and are therefore considered more accurate. Thus the LOX post 1L mode is predicted to fall in the range 6.3–6.7 kHz and the 2L from 12.8–13.3 kHz.

Table 3. Estimated LOX post mode frequencies.

Method	Eq. 4	Exp. based[13)]	FEA	NM
f_{1L} [Hz]	7130	7070	6630	6390
f_{2L} [Hz]	14250	13580	13250	12880

4.3. Coupling analysis

The frequencies of the LUMEN combustion chamber modes were estimated with Eq. 2. The combustion efficiency was chosen as 95% and the baseline geometry of the combustion chamber is $R = 40$ mm and $L = 307$ mm with a contraction ratio of $\epsilon_c = 2.3$. The effective speed of sound factors k_l and k_t are determined using in-house and published axial c_{CC} profiles.[5,15,29] The combustion zone was assumed to be 25% of the chamber length. The resulting frequencies for some modes are presented in Tab. 4.

Table 4. Estimated LUMEN chamber mode frequencies according to Eq. 2

Chamber mode	Frequency [Hz]
1L	1610
1T	5040
1T1L	6290
1T2L	6730
2T	8360
1R	10490

The calculated transverse mode frequencies are around 40% lower than with Eq. 1 and a constant value of $c_{CC,CEA}$. While this difference seems extreme, the approach with Eq. 2 was validated with test data from another DLR combustor of similar scale operated with LOX/LNG and shear coaxial injectors. The significant impact on transverse modes illustrates the importance of a detailed model of the acoustic field in the chamber.

Predicted frequencies for the combustion chamber and injector modes can now be compared for their potential to couple and mutually amplify. The fundamental LOX post mode (1L) lies above both the fundamental chamber modes 1L and 1T, which precludes the most dangerous coupling combinations, and should be between the chamber 1T1L and 1T2L modes. In the range of the LOX post 2L mode there are only higher order combination modes in the chamber, which are typically better damped than the primary modes. Based on the results of this analysis the design should be robust with respect to injection-coupled instabilities. However, the acoustic models of both the post and the chamber need to be verified by experimental data after the initial tests with the LUMEN injector head at the P8 test bench.

A key requirement in the design of expander cycle engines is the extraction of sufficient enthalpy from the thrust chamber cooling circuit to drive the turbines. Since a P8 test campaign to measure the heat flux profile of the LUMEN injector head with a calorimetric combustion chamber is currently in progress, the length of the LUMEN combustion chamber may change from the baseline design. For that reason a parametric sweep of the chamber length in the chamber acoustic analysis has been performed with the goal of identifying lengths which should be avoided based on potential coupling with the LOX post modes.

The chamber length was varied between 250 and 460 mm. Fig. 10 shows the frequencies of the longitudinal chamber modes (1L to 10L) compared to the LOX post 1L and 2L frequencies. For the baseline chamber length of 307 mm, the LOX post 2L and chamber 9L have similar frequencies. However, it is generally assumed that higher order longitudinal modes are more highly damped and therefore a significant excitation of this mode is not expected. For various other chamber lengths, the LOX post 1L mode coincides with the chamber 4L, 5L, or 6L. From this analysis is was concluded that chamber lengths of 250 mm, 340–350 mm, and around 420 mm have the potential to drive chamber longitudinal modes and should be avoided if possible.

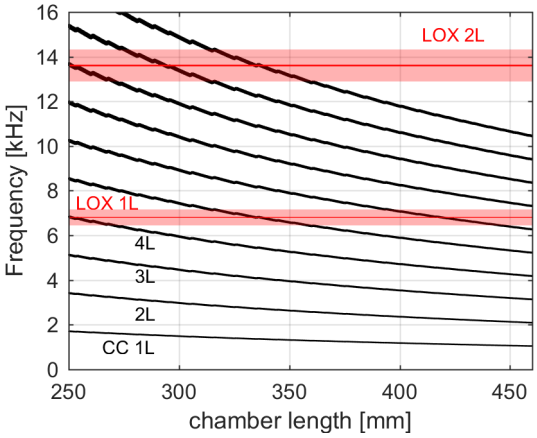

Fig. 10. Chamber longitudinal mode frequency dependence on chamber length, compared with LOX injector modes.

5. Low frequency stability

Low-frequency (LF) instabilities can also have a major impact on the safe operation of LREs. Therefore the LUMEN injector head design was analysed to investigate the potential for oscillatory coupling between the combustion chamber and injector head.

5.1. Low-frequency stability model

A common approach to predict LF instabilities is the refined time-lag model of Crocco,[7] which approximates the response of the combustion processes to varying inflow conditions as a single time delay τ and interaction index n. One of the most significant developments of this approach was the division of the total time lag τ_t into the insensitive time-lag τ_i, which is not affected by operating conditions of the combustion chamber, and the sensitive time-lag τ_s, which varies with different chamber conditions such as temperature and pressure. The extent of the influence on the combustion processes is described by the interaction index n. The modelling approach describes the combination of feed lines and combustion chamber as a coupled system of oscillators according to control theory. Knowing the transfer function $G(i\omega)$ therefore enables the dynamic response $Y(i\omega)$ of a given input $X(i\omega)$ to be calculated according to

$$G(s) = \frac{Y(s)}{X(s)}. \tag{7}$$

Based on the conservation of mass for the combustion chamber, the transfer function of the combined feed and combustion chamber system can be expressed as

$$\frac{\dot{m}_b(t)}{\bar{\dot{m}}_{tot}} = \frac{\dot{m}_e(t)}{\bar{\dot{m}}_{tot}} + \frac{1}{\bar{\dot{m}}_{tot}} \frac{d}{dt} M_g(t). \tag{8}$$

Here, $\dot{m}_b$ describes the mass flow of burned propellants, $\dot{m}_e$ the mass flow of cumbustion products exiting through the nozzle,

and M_g the fraction of gases remaining in the combustion chamber. Equation 8 is further normalized by the total massflow $\bar{m}_{tot}$. Following Casiano[4] and Crocco,[7] Eq. 8 can be stated more precisely as

$$
\begin{aligned}
0 = 1 &+ \theta_g s - n \cdot (1 - e^{-s\tau_s}) \\
&+ \left[\frac{1}{2} \left(\frac{\overline{T}_b}{\overline{\dot{m}}_b \overline{T}_b} \overline{\dot{m}}_{ox} \right.\right. \\
&+ \frac{\overline{\dot{m}}_{ox} + \overline{\dot{m}}_f}{\overline{\dot{m}}_b \overline{T}_b} \overline{ROF} \left(\frac{dT_b}{dROF} \right)_n \Big|_{\overline{ROF}} \Big) e^{-s(\theta_g + \tau_s)} \\
&- \Big(\frac{\overline{T}_b}{\overline{\dot{m}}_b \overline{T}_b} \overline{\dot{m}}_{ox} \\
&+ \frac{\overline{\dot{m}}_{ox} + \overline{\dot{m}}_f}{\overline{\dot{m}}_b \overline{T}_b} \overline{ROF} \left(\frac{dT_b}{dROF} \right)_c \Big|_{\overline{ROF}} \Big) e^{-s\tau_s} \\
&\left. - \frac{\overline{\dot{m}}_{ox}}{\overline{\dot{m}}_{tot}} e^{-s\tau_t} \right] G_{ox}(s) \\
&+ \left[\frac{1}{2} \left(\frac{\overline{T}_b}{\overline{\dot{m}}_b \overline{T}_b} \overline{\dot{m}}_f \right.\right. \\
&- \frac{\overline{\dot{m}}_{ox} + \overline{\dot{m}}_f}{\overline{\dot{m}}_b \overline{T}_b} \overline{ROF} \left(\frac{dT_b}{dROF} \right)_n \Big|_{\overline{ROF}} \Big) e^{-s(\theta_g + \tau_s)} \\
&- \Big(\frac{\overline{T}_b}{\overline{\dot{m}}_b \overline{T}_b} \overline{\dot{m}}_f \\
&- \frac{\overline{\dot{m}}_{ox} + \overline{\dot{m}}_f}{\overline{\dot{m}}_b \overline{T}_b} \overline{ROF} \left(\frac{dT_b}{dROF} \right)_c \Big|_{\overline{ROF}} \Big) e^{-s\tau_s} \\
&\left. - \frac{\overline{\dot{m}}_f}{\overline{\dot{m}}_{tot}} e^{-s\tau_t} \right] G_f(s).
\end{aligned}
\tag{9}
$$

Here, θ_g represents the residence time in the chamber, T_b the temperature of the burnt propellants, $\overline{\dot{m}}_{ox}$ the oxidizer and $\overline{\dot{m}}_f$ the fuel mass flow rates. The indices n and c describe the state at the nozzle entrance and combustion front. Modelling of the transfer function G_{ox} for the oxidizer and G_f for the fuel feeding systems is done with a lumped-parameter approach based on a serial connection of the transfer functions of the building blocks found in Harrje and Reardon.[17]

5.2. Stability analysis

For the model of the LUMEN thrust chamber and supply system, τ_t was chosen to be the residence time of the gases in the combustion chamber. In previous post-test modelling of LF instabilities in DLR combustors, this choice of time lag resulted in good agreement with the experimentally observed frequencies and stability characteristics.

Due to the lack of a transfer function for a porous injector, the analysis was restricted to the LOX injection and supply system. To keep the bi-propellant formulation of the model but exclude the influence of porous injector dynamics, an artificially high pressure drop was introduced on the fuel side which suppresses its influence on the system response.

The model was solved for a range of p_{CC} and ROF extending below the specified LUMEN envelope. For each LP, values of τ_i, τ_s, and n were swept within reasonable limits. If instabilities were predicted for any combination of these values, the LP was labelled as unstable. Figure 11 shows the resulting stability map with respect to p_{CC} and ROF. LF instabilities are possible in the low p_{CC} and ROF ranges where LOX injection pressure drop is also low, but the nominal LP at 60 bar, ROF 3.4 is expected to be stable.

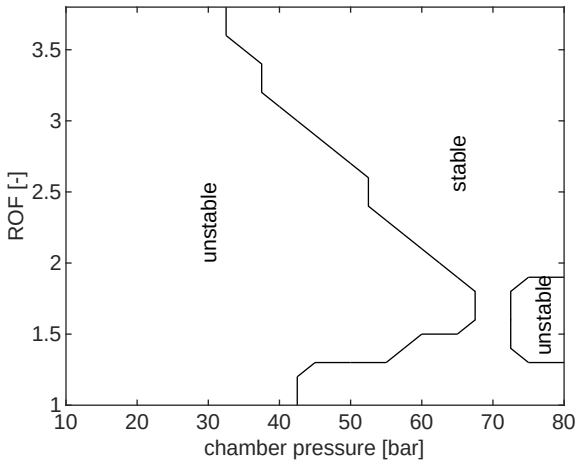

Fig. 11. Predicted low-frequency stability boundaries with respect to p_{CC} and ROF

6. Summary and outlook

The design of an injection system for the LUMEN demonstrator engine with LOX/LNG was presented. The main aspects of the design treated in this article were the distribution of LOX among the injection posts, and the consideration of both high and low frequency combustion instabilities. The propellant distribution was predicted with CFD, and the acoustic modes of the injector and combustion chamber were estimated with FEA and low-order modelling methods. Low frequency stability was predicted with a model of the coupled injection-chamber system following the Crocco $n - \tau$ approach.

A campaign to test the ignition transient and stationary operating characteristics of this new injector head is currently underway at the European Research and Technology Test Facility P8 for cryogenic rocket engines at DLR Lampoldshausen. When the test data are available, the measured characteristics of the injector will be compared to the predicted values, for example injection pressure drop and acoustic mode frequencies, and the combustion efficiency will be assessed with respect to the project requirements.

References

1) Armbruster, W., Hardi, J. S., Suslov, D., and Oschwald, M. Experimental investigation of self-excited combustion instabilities with injection coupling in a cryogenic rocket combustor. *Acta Astronautica 151* (October, 2018), 655–667.
2) Börner, M., Deeken, J. C., Manfletti, C., and Oschwald, M. Experimental study of a laser ignited thruster with a porous injector head. *International Journal of Energetic Materials and Chemical Propulsion* (2019).
3) Börner, M., Manfletti, C., Hardi, J. S., Suslov, D., Kroupa, G., and Oschwald, M. Laser ignition of a multi-injector lox/methane combustor. *CEAS Space Journal 10* (2018), 273–286.
4) Casiano, M. *Extensions to the Time Lag Models for Practical Apllication to Engine Stability Design*. PhD thesis, The Pennsylvania State University, 2010.

5) Chemnitz, A., and Sattelmayer, T. Acoustic characterization of virtual thrust chamber demonstrators. In *Sonderforschungsbereich/Transregio 40 Annual Report 2018* (2018), DFG, pp. 169–180.
6) Chen, P., Nie, W., Guo, K., amd Yu Liu, X. S., and Wang, H. The effects of non-uniform distribution of oxidizer flow on high-frequency combustion instability. *MATEC Web of Conferences 257, 01005* (2019).
7) Crocco, L. Aspects of combustion stability in liquid propellant rocket motors part II: Low frequency instability with bipropellants. high frequency instability. *Journal of the American Rocket Society 22*, 1 (jan 1952), 7–16.
8) Deeken, J., Oschwald, M., and Schlechtriem, S. Lumen demonstrator - project overview. In *Space Propulsion 2018* (Seville, Spain, 2018).
9) Deeken, J., Oschwald, M., and Schlechtriem, S. Lumen demonstrator - project overview. In *32nd International Symposium on Space Technology and Science* (Aochi, Japan, 2019).
10) Deeken, J., S. D. R. N., and Preuss, A. Combustion performance and stability of a porous injector compared with a state-of-the-art coaxial injector. In *Space Propulsion 2014* (Cologne, Germany, 2014).
11) Dranovsky, M. L., Ed. *Combustion Instabilities in Liquid Rocket Engines: Testing and Development Practices in Russia*. Progress in Astronautics and Aeronautics, 2007.
12) Gröning, S. *Untersuchung selbsterregter Verbrennungsinstabilitten in einer Raketenbrennkammer*. PhD thesis, RWTH Aachen, Aachen, Germany, 2017.
13) Gröning, S., Hardi, J. S., Suslov, D., and Oschwald, M. Injector-driven combustion instabilities in a Hydrogen/Oxygen rocket combustor. *Journal of Propulsion and Power 32*, 3 (2016), 560–573.
14) Gröning, S., Suslov, D., Oschwald, M., and Sattelmayer, T. Stability behaviour of a cylindrical rocket engine combustion chamber operated with liquid hydrogen and liquid oxygen. In *5th European Conference for Aeronautics and Space Sciences (EUCASS) 2013* (Munich, Germany, 2013).
15) Hardi, J. S., Kaess, R., Tonti, F., Blanco, P. N., Soller, S., Oschwald, M., Gernoth, A., and De Rosa, M. Study of the influence of operating conditions on lox/h2 thrusth chamber acoustic eigenmodes. In *Space Propulsion 2018* (Seville, Spain, 2018).
16) Hardi, J. S., Oschwald, M., and Dally, B. B. Acoustic characterisation of a rectangular rocket combustor with liquid oxygen and hydrogen propellants. *Proceedings of the Institution of Mechanical Engineers, Part G: Journal of Aerospace Engineering 227*, 3 (mar 2013), 431–441.
17) Harrje, D., and Reardon, F., Eds. *Liquid Propellant Rocket Combustion Instability* (1972), NASA SP-194.
18) Huber, W. *Impact of Fuel Supply Impedance on Combustion Stability of Gas Turbines*. PhD thesis, Technische Universität München, München, Germany, 2009.
19) Hulka, J. R., and Jones, G. W. Performance and stability analyses of rocket thrust chambers with oxygen/methane propellants.
20) Hutt, J. J., and Rocker, M. High-frequency injection-coupled combustion instability. In *Liquid Rocket Engine Combustion Instability*, V. Yang and W. E. Anderson, Eds. American Institute of Aeronautics and Astronautics, Washington, DC, 1995, ch. 12, pp. 345–356.
21) Jensen, R. J., Dodson, H. C., and Claflin, S. E. *LOX/Hydrocarbon Combustion Intability Investigation*. NASA CR 182249. NASA Lewis Research Center, 1989.
22) Kawashima, H., Kobayashi, K., and Tomita, T. A combustion instability phenomenon on a LOX/Methane subscale combustor. In *46th AIAA/ASME/SAE/ASEE Joint Propulsion Conference & Exhibit 2010* (AIAA Paper 2010-7082, Nashville, Tennessee, 2010).
23) Lemmon, E. W., Huber, M. L., and McLinden, M. O. Nist standard database 23. nist reference fluid thermodynamic and transport properties–refprop, version 9.1 (national institute of standards and technology, standard reference data program, gaithersburg), 2013.
24) Lux, J., Suslov, D., and Haidn, O. J. On porous liquid propellant rocket engine injectors. *Aerospace Science and Technology 12*, 6 (sep 2008), 469–477.
25) Melcher, J. C., and Morehead, R. L. Combustion stability characteristics of the project morpheus liquid oxygen / liquid methane main engine. In *50th AIAA/ASME/SAE/ASEE Joint Propulsion Conference & Exhibit 2014* (AIAA Paper 2014-3681, Cleveland, Ohio, 2014).
26) Nunome, Y., Onodera, T., Sasaki, M., Tomita, T., Kobayashi, K., and Daimon, Y. Combustion instability phenomena observed during cryogenic hydrogen injection temperature ramping tests for single coaxial injector elements. In *47th AIAA/ASME/SAE/ASEE Joint Propulsion Conference & Exhibit 2011* (AIAA Paper 2011-6027, San Diego, California, 2011).
27) Nunome, Y., Takahashi, M., Kumakawa, A., Miyazaki, K., Yoshida, S., and Onga, T. High-frequency flame oscillation observed at a coaxial lox/lh2 injetor element. In *44th AIAA/ASME/SAE/ASEE Joint Propulsion Conference & Exhibit 208* (AIAA Paper 2008-4848, Hartfort, Connecticut, 2008).
28) Polifke, W., van der Hoek, J., and Verhaar, B. Everything you always wanted to know about f and g. *Technische Universität München, München, Germany* (1997).
29) Schulze, M., and Sattelmayer, T. Linear stability assessment of a cryogenic rocket engine. In *Thermoacoustic Instabilities in Gas turbines and Rocket Engnines: Industry meets Academia 2016* (Munich, Germany, 2016).
30) Suslov, D., Lux, J., and Haidn, O. Investigation of porous injector elements for lox/ch4 and lox/h2 combustion at sub- and supercritical conditions. In *2nd European Conference for Aeronautics and Aerospace Sciences (EUCASS) 2017* (Brussels, Belgium, 2007).
31) Urbano, A., Selle, L., Staffelbach, G., Cuenot, B., Schmitt, T., Ducruix, S., and Candel, S. Exploration of combustion instability triggering using large eddy simulation of a multiple injector liquid rocket engine. *Combustion and Flame 169* (July 2016), 129–140.
32) Watanabe, D., Manako, H., Onga, T., Tamura, T., Ikeda, K., and Isono, M. Combustion stability improvement of le-9 engine for booster stage of h3 launch vehicle. *Mitsubishi Heavy Industries Technical Review 53* (2016), 28–35.
33) Yang, V., and Anderson, W., Eds. *Liquid Rocket Engine Combustion Instability*. American Institute of Aeronautics and Astronautics, Washington, DC, 1995.